Polymer Journal (2012) 44, 706–712

www.nature.com/pj

ORIGINAL ARTICLE

Influence of magic angle spinning on T_1^H of SBR studied by solid state ^{1}H NMR

Atsushi Asano, Shunsuke Hori, Masashi Kitamura, Chikako T Nakazawa and Takuzo Kurotsu

We have investigated the influence of the high centrifugal pressure caused by fast magic-angle spinning (MAS) on the molecular motion of styrene–butadiene rubbers (SBR) filled with SiO_2 (SBR/Si composite) though solid-state magic-angle spinning nuclear magnetic Resonance (^{1}H MAS NMR) measurements. Because the ^{1}H–^{1}H dipolar interaction of elastomers is weak compared with that of glassy polymers, a narrower ^{1}H linewidth is observed under fast MAS. The temperature dependence of the ^{1}H spin-lattice relaxation time (T_1^H) revealed that the T_1^H minimum increases with the MAS rate. Furthermore, we observed a difference in the temperature dependence of T_1^H between end-chain-modified SBR and normal (unmodified) SBR in the SBR/Si composites. The temperature dependence of T_1^H is described by the Bloembergen–Purcell–Pound theory, with the assumption that the correlation time obeys the Williams–Landel–Ferry empirical theory. The fitting showed that the molecular motion does not change significantly until a MAS rate of 20 kHz, with the motional mode changing considerably at a MAS rate of 25 kHz. The motion of SBR in the unmodified SBR/Si composite was greatly affected by the fast MAS rates. Furthermore, the plot of the estimated centrifugal pressure versus the T_1^H minimum resembled the stress–strain curve. This result enables the detection of macroscopic physical deformation by the microscopic parameter T_1^H.
Polymer Journal (2012) **44,** 706–712; doi:10.1038/pj.2012.10; published online 7 March 2012

Keywords: centrifugal pressure; ^{1}H spin-lattice relaxation time; molecular motion; Payne effect; solid-state ^{1}H NMR linewidth

INTRODUCTION

Solid-state NMR is useful for the investigation of the molecular motion of the functional groups of elastomers and polymers. In particular, the recent development of the magic-angle spinning (MAS) technique allows a sample rotor to be spun much faster than 20 kHz. Thus, we can detect the high-resolution ^{1}H signals of rubbers and elastomers under the fast rates that are possible in MAS because these fast MAS rates effectively reduce the signal broadening that arises from the relatively weak ^{1}H–^{1}H dipolar interaction of elastomers (in comparison with that of glassy solid polymers).

Generally, spin-lattice relaxation time (T_1) is observed to study molecular motion. In the case of rare spins such as ^{13}C, however, it is time-consuming to observe the signals and measure an accurate T_1 with a good signal-to-noise ratio. In contrast, proton signals are intense enough to allow quick analysis of molecular motion through the T_1 measurement. However, for a glassy solid polymer, the strong ^{1}H–^{1}H dipolar interaction obscures the individual functional group signals, even with fast MAS. For rubbers and elastomers under fast MAS, in contrast, each peak assigned to a respective functional group can be detected because of the weak ^{1}H–^{1}H dipolar interaction. Furthermore, it is easy to detect ^{1}H–T_1 (^{1}H spin-lattice relaxation time (T_1^H)) accurately.

In contrast, it is well known that MAS causes the temperature of the inner sample to increase because of friction between the MAS and the air. In addition, it has recently been reported that fast MAS causes structural changes and motional change in membrane proteins through centrifugal pressure.[1,2] Therefore, it is important to clarify the influence of MAS on the ^{1}H spectra and T_1^H so that the actual molecular motion of the elastomers can be understood.

In this study, we measured the temperature dependence of T_1^H to investigate molecular motion under various MAS conditions. To examine the effect of pressure, we obtained T_1^H under several MAS rates using two types of sample rotors with outer diameters of 3.2 and 6.0 mm. The actual temperature around the sample was also calibrated by the methanol[3] and lead nitrate[4] methods under MAS.

EXPERIMENTAL PROCEDURE

Samples

The materials used were two types of styrene–butadiene rubber (SBR) with SiO_2 (SBR/SiO_2) composites, which were provided by the YOKOHAMA rubber Co. Ltd (Kanagawa, Japan) through the Advanced Elastomer research group in the Society of Rubber Industry, Japan. One material was a normal SBR (*n*-SBR), and the other was modified at the end-chain by an alkoxysilyl group (*em*-SBR).[5] The fundamental formulations of both SBR/SiO_2 composites were 50 parts per hundred rubber (phr) of SiO_2, 5 phr of bis-(3-(triethoxysilyl)propyl)tetrasulfide, 3 phr of ZnO, 1 phr of stearic acid, 1 phr of *N*-phenyl-*N*′-1,3-dimethylbutyl-p-phenylendiamine as an antioxidant, 15 phr of aromatic oil, 2 phr of sulfur, 2 phr of *N*-cyclohexyle-2-benzothiazylsulfenamide and 0.7 phr of diphenylguanidine per 100 parts by weight of SBR; for example, 50 phr of SiO_2 means 50 parts by weight of SiO_2

Department of Applied Chemistry, National Defense Academy, Yokosuka, Kanagawa, Japan
Correspondence: Dr A Asano, Department of Applied Chemistry, National Defense Academy, Hashirimizu 1-10-20, Yokosuka, Kanagawa 239-8686, Japan.
E-mail: asanoa@nda.ac.jp.
Received 20 September 2011; revised 5 December 2011; accepted 31 December 2011; published online 7 March 2012

per 100 parts by weight of SBR. Both composites were vulcanized by pressing at 160 °C for 12 min. Anhydrous methanol was purchased from Kanto Chemical Co. Inc (Tokyo, Japan), and lead nitrate of extra pure grade was obtained from Wako Pure Chemical Industries, Ltd (Osaka, Japan).

Nuclear magnetic resonance measurements

High-resolution solid-state ^{1}H NMR measurements were made using a Varian NMR system spectrometer (Agilent Technologies, Santa Clara, CA, USA) operating at 399.94 MHz at several MAS speeds (2–9 kHz for a 6.0-mmϕ rotor and 5–25 kHz for a 3.2-mmϕ rotor). The MAS speed was controlled within ± 20 Hz at a set rate. The proton chemical shifts were measured in reference to tetramethylsilane and the spin-lattice relaxation times in the laboratory frame (T_1^H) were measured by the conventional inversion-recovery method.

The actual temperature at which the sample was kept was calibrated mainly by the classical methanol method under MAS,[3] and the lead nitrate method[4] was partly used to estimate the actual temperature. Anhydrous methanol was sealed in a rotor with an o-ring cap for a 6.0-mmϕ sample rotor. For the 3.2-mmϕ sample rotor, we used a small piece of polyurethane rubber as a cap to prevent leakage of methanol under the MAS because the o-ring cap was not provided for the 3.2-mmϕ sample rotor. The temperature was regulated by dried and compressed air, which was differentiated from the bearing air and the spinning air used to rotate the sample rotor. The variable temperature experiments were performed after the temperature was stabilized and maintained for 15 min.

Differential scanning calorimetry measurements

Differential scanning calorimetry was performed using a Perkin–Elmer 7 system, in which the temperature was increased at the rate of 2 K min^{-1} from 213 to 393 K.

RESULTS AND DISCUSSION

^{1}H MAS spectra of SBR

Figure 1 shows the solid-state ^{1}H MAS NMR spectra of the *em*-SBR/Si composite at MAS speeds of 5, 10, 15, 20 and 25 kHz at a regulated temperature of 298 K. Because of the friction between the rotating MAS rotor and the air, the temperature inside the rotor tended to rise, even though the temperature was controlled. The calibrated temperatures at each MAS rate were 299, 303, 309, 317 and 327 K, respectively. At a MAS speed of 25 kHz, the ^{1}H MAS NMR spectrum provided well-resolved peaks that consisted of three types of protons, namely the benzene ring protons (~7 p.p.m.), the double-bonded methine (CH) and methylene (CH_2) protons (~5 p.p.m.) and the single-bonded methylene and methyl protons (~2 p.p.m.). As the MAS speed was reduced, the ^{1}H NMR spectrum became broader, and the signal intensity decreased. Even at 5 kHz MAS, however, each ^{1}H NMR signal was distinguishable. The broadening was caused by the residual ^{1}H–^{1}H dipolar interaction, which is not eliminated by the slow MAS rate of 5 kHz.

Magic-angle spinning is usually used to eliminate the chemical shift anisotropy in the solid state. Because the chemical shift anisotropy interaction has a term of $(3\cos^2\theta - 1)$ in which θ is the angle between the static magnetic field and the nuclear spin magnetization, the overall average of the term becomes zero during MAS ($= \cos^{-1}(1/3)^{0.5}$). The chemical shift anisotropy disappears and becomes the isotropic chemical shift. The ^{1}H–^{1}H dipolar interaction has the same term; therefore, MAS can reduce the dipolar interaction when its strength is weak enough to be eliminated by the MAS rate. Figure 1 shows that a MAS speed of 5 kHz is too slow to reduce the ^{1}H dipolar interaction effectively. This result implies that the strength of the ^{1}H–^{1}H dipolar interaction is of the order of a few tens of kHz at 315 K. The actual temperature also rises as the MAS rate increases. Consequently, the molecular motion of the SBR becomes faster, and the ^{1}H–^{1}H dipolar interaction becomes weaker than at room temperature. Therefore, the increased sharpness and signal intensity

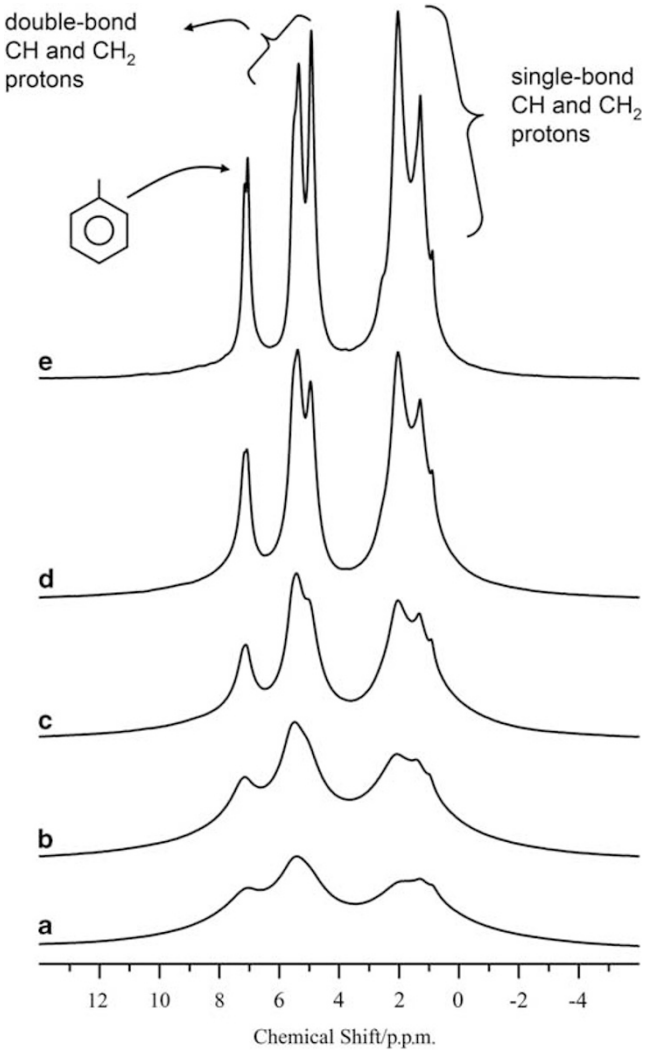

Figure 1 Solid-state ^{1}H MAS NMR spectra of the *em*-SBR/Si composite at a regulated temperature of 298 K. The MAS rate was (**a**) 5 kHz, (**b**) 10 kHz, (**c**) 15 kHz, (**d**) 20 kHz and (**e**) 25 kHz. The calibrated (actual) temperatures were 299, 303, 309, 317 and 327 K, respectively.

are caused by the mixed effects of an increase in the MAS speed and the weakened ^{1}H–^{1}H dipolar interaction. To investigate and distinguish the effects of both MAS and temperature on the linewidth, we observed ^{1}H MAS NMR spectra as the calibrated temperature became constant, even at different MAS rates. For example, we can discuss the difference in the MAS effect between the ^{1}H MAS NMR spectra at MAS rates of 5 and 10 kHz at the same calibrated temperature. In this case, of course, the regulated temperature at a MAS rate of 5 kHz is different from that at a MAS rate of 10 kHz. For the unmodified *n*-SBR/Si composite, similar results were also obtained.

Figure 2 shows the ^{1}H MAS NMR spectra of the *em*-SBR/Si composite at 360 K. The temperature shown is the calibrated value; each controlled temperature is different from the others. It is clear that both the double- and single-bonded CH/CH_2 signals became drastically narrower and higher at resonance. Furthermore, the spectral resolution at a MAS rate of 5 kHz is comparable to that at a MAS rate of 25 kHz. This similarity occurs because the molecular motion of the SBR becomes highly active at such a high temperature, and the ^{1}H–^{1}H dipolar interaction becomes so weak as to be negligible. This observation suggests that the strength of the ^{1}H–^{1}H

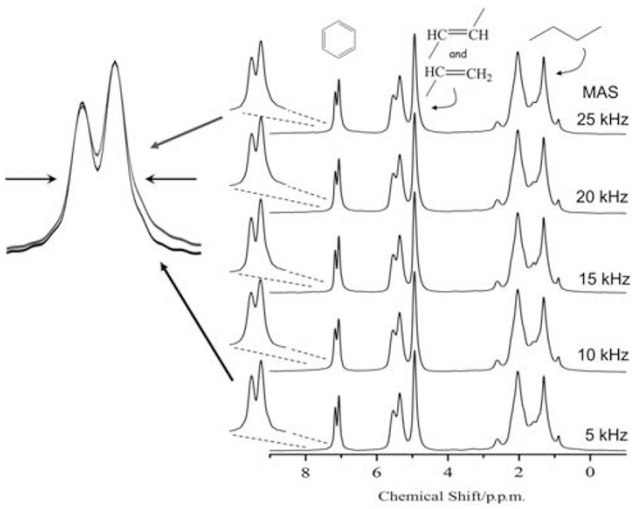

Figure 2 Solid-state ^{1}H MAS NMR spectra of the *em*-SBR/Si composite at actual temperature of 360 K.

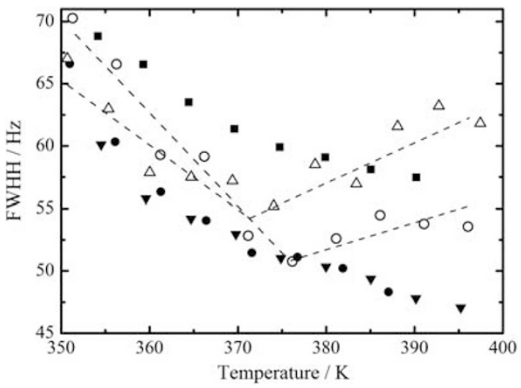

Figure 3 Full linewidth at half height (FWHH) of the benzene ring signal (~7 p.p.m.) versus the calibrated temperature for the *em*-SBR/Si composite at MAS speeds of 5 (●), 10 (■), 15 (▼), 20 (○) and 25 kHz (△). The broken lines are depicted as guides.

dipolar interaction becomes weaker than a few kHz at 360 K. Therefore, MAS effectively eliminates the ^{1}H–^{1}H dipolar interaction.

Interestingly, the linewidths of peaks in Figure 2 do not decrease as the MAS speed increases, as can be observed from the benzene ring peak (enlarged figure). The expanded spectra in the region of the benzene ring are also shown in Figure 2. Clearly, the splitting of the peak at a MAS rate of 5 kHz appears to narrow much more than those at MAS rates of 10, 20 or 25 kHz. The enlarged spectra at 5 and 25 kHz MAS rates are also shown in the left-hand side for comparison. The comparison clearly shows that the linewidth at a MAS rate of 25 kHz becomes broader than that at a MAS rate of 5 kHz. On the other hand, the signals in the regions of the single- and double-bonded CH and CH_2 protons show similar linewidths at each MAS rate. In general, the resolution of the NMR spectrum improves with increasing MAS speed, as stated above. Therefore, the constancy of the linewidth is attributed to the weakened ^{1}H–^{1}H dipolar interaction. A MAS rate of 5 kHz is adequate to eliminate the effect of the ^{1}H–^{1}H dipolar interaction on the linewidth.

To investigate the relationship between the MAS rate and the resolution, we measured the full linewidth at half height (FWHH) of the benzene ring signal. The increase of the FWHH is attributable to the fact that the molecular motion becomes slow and hindered. Figure 3 shows the relationship between the FWHH and the temperature at MAS speeds from 5 to 25 kHz. The FWHH values observed at 5 (●) and 15 kHz (▼) MAS decrease similarly with temperature. The FWHH values at 10 kHz (■) MAS are larger than those at 5 and 15 kHz MAS, but it decreases similarly with temperature. Figure 2 also shows that the ^{1}H benzene peak observed at a MAS rate of 10 kHz is broader than those at MAS rates of 5 and 15 kHz. It is well known that resonance peak broadening occurs in the case of ^{13}C observation with ^{1}H–^{13}C dipolar decoupling because of the interference between the strength of the radio-frequency irradiation and the molecular motion.[6–8] The similar frequency of the molecular motion and the radio-frequency irradiation reduces the efficiency of the decoupling. Because radio-frequency irradiation is not employed for ^{1}H measurements, the broadening observed at 10 kHz MAS is presumably ascribed to the interference between the strength of the ^{1}H–^{1}H dipolar interaction and the MAS rate. This interference causes the loss of the ^{1}H–^{1}H dipolar decoupling efficiency at 10 kHz MAS, and it leads to the recoupling of the ^{1}H–^{1}H dipolar interaction. This result suggests that the molecular motion of the *em*-SBR in the silica composite becomes slow, and the recoupled ^{1}H–^{1}H dipolar interaction has a frequency range of ~10 kHz at higher temperatures. On the other hand, the *n*-SBR in the silica composite did not show such broadening, and the linewidth was comparable to that at 5 and 15 kHz MAS. This result indicates that the *em*-SBR interacts with the silica, and the molecular motion is slowed with respect to that of the *n*-SBR in the silica composite.

For the spectra at MAS rates of 20 (○) and 25 kHz (△), the FWHH values decrease in the same manner as those obtained at MAS rates of 5–15 kHz at temperatures <375 K. However, the FWHH values increase at temperatures >375 K for MAS rates of both 20 and 25 kHz. This trend indicates that the molecular motion becomes slow, even at higher temperatures. In general, the molecular motion of polymers becomes faster with increasing temperature. Similarly, the molecular motion of the SBR becomes active at temperatures >380 K. This result contradicts to the observation of narrowing with increasing temperature. One may wonder whether further vulcanization or a cross-linking reaction occurs at these higher temperatures. We have checked the temperature dependence of the linewidth for the sample after increasing the temperature to nearly 400 K, and we obtained the same temperature dependence as that shown in Figure 3. If such a reaction occurs at ~400 K, the temperature dependence of the second experiment should have changed.

We observed two interesting and characteristic phenomena. One is the signal broadening at a MAS rate of 10 kHz over the entire temperature range. The other is the increase of the signal linewidth at temperatures >375 K for MAS rates of both 20 and 25 kHz. The former phenomenon can be interpreted to indicate the interference between the molecular motion and the MAS frequency, as stated above. However, there is an argument that the molecular motion of the benzene ring keeps the frequency ~10 kHz at the temperature range from 350 to 400 K. The FWHH becomes large in the case of higher temperatures at MAS rates of 20 and 25 kHz. We should consider the existence of a centrifugal force generated by the fast MAS in the rotor because the softened materials are easily deformed by the force. The fast MAS causes strong enough centrifugal force (inner pressure) to effectively hinder the molecular motion of rubbers and elastomers. The pressure P (Pa), can be calculated from the MAS speed k (Hz), the inner radius of the rotor r (m) and the sample

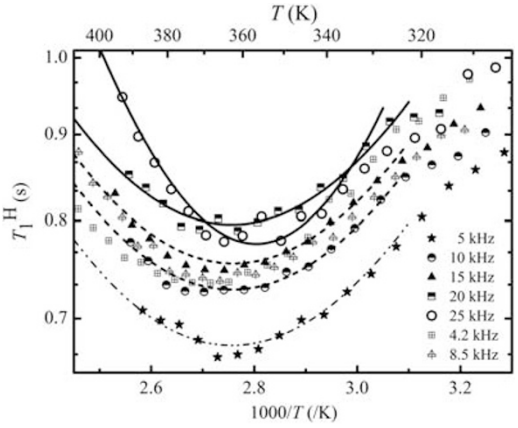

Figure 4 Observed T_1^H values at the benzene ring proton signals against the inverse of temperature (1/*T*) for the *n*-SBR/Si composite. The vertical axis is on a logarithmic scale. The solid, dashed and two-dotted dashed lines are the theoretical T_1^H curves obtained from the combination of Equations (2) and (3).

density ε (kg m^{-3}) by the following equation[1,2] (Private discussions with Dr Kawamura and Prof Naito of Yokohama National University (refs 1 and 2). Centrifugal force F can be estimated from $F = mr\omega^2 = \int_0^{\pi}\int_0^{2\pi} (rd\theta \cdot dr \cdot l \cdot \varepsilon) \cdot r \cdot (2\pi k)^2 = 8\pi^3 k^2 r^3 l\varepsilon / 3$. The pressure P is obtained from F/S; S is the area of inner rotor, $2\pi rl$ (a cylinder with an inner radius of r and a length of l)):

$$P = \frac{4}{3}\pi^2 k^2 r^2 \varepsilon. \tag{1}$$

From Equation (1), the pressures at MAS rates of 20 and 25 kHz can be estimated to be 6.1 and 9.5 MPa, respectively; the sample density was $\sim$1150 kg m^{-3}. At MAS speeds of 5, 10 and 15 kHz with a 3.2-mmϕ rotor (r = 1 mm), the values were calculated to be 0.4, 1.5 and 3.4 MPa, respectively. This simple calculation indicates that the inner pressure is very high at MAS rates >20 kHz. The pressure value of several MPa is large enough to affect the molecular motion of rubbers and elastomers, but it is not sufficient to cause a deformation of general solid polymers.

From the viewpoint of the pressure, the molecular motion of the SBR/Si composites is affected by the pressure, according to the MAS rate. The molecular motion under pressure is slower than the motion under normal conditions. This effect allows the ^{1}H–^{1}H dipolar interaction, which is reduced by MAS, to be restored to some extent. If the residual dipolar interaction is weak enough, the observed ^{1}H MAS NMR spectrum does not broaden. However, broadening is observed when the recoupled dipolar interaction is close to the MAS rate. For the *em*-SBR/Si composite, the FWHH is broader than that of the *n*-SBR/Si composite at a MAS rate of 10 kHz, as stated above. Although the SBR is affected by the same pressure, the strength of the dipolar interaction of the *em*-SBR is larger than that of the *n*-SBR. This difference indicates again that the molecular motion of the *em*-SBR is slower than that of the *n*-SBR in the silica composites. There exists an interaction between the *em*-SBR and the silica via the end-chain-modified functional group. At much slower MAS rates and higher temperatures, the small pressure does not influence the molecular motion; thus, there is little change of the FWHH for either *em*-SBR or *n*-SBR. In contrast, at much faster MAS rates, the strength of the recoupled ^{1}H–^{1}H dipolar interaction becomes larger than the MAS rate, and results in broadening of the spectrum.

Temperature dependence of T_1^H

Figures 2 and 3 show the change of the molecular motion of SBR in silica composites under various MAS conditions through a linewidth analysis. If the molecular motion changes significantly, the T_1^H is also affected. To investigate the effect of pressure on T_1^H, we observed the temperature dependence of T_1^H at various MAS rates, as shown in Figure 4. For this experiment, we used two sample rotors with diameters of 3.2 and 6.0 mm. In addition, the MAS rates of the 6.0 mmϕ rotor were chosen to produce the same pressure as that produced by the 3.2 mmϕ rotor. For example, the pressure at 4.2 kHz MAS with a 6.0-mmϕ rotor is equal to the pressure produced by a 3.2-mmϕ rotor at 10 kHz MAS (1.5 MPa), 8.5 kHz MAS with a 6.0-mmϕ rotor corresponds to 20 kHz MAS (6.1 MPa) with a 3.2-mmϕ rotor, and so on. Figure 4 shows the temperature dependence of T_1^H of the benzene ring protons for the *n*-SBR/Si composite. Similar temperature dependencies were also observed for the *em*-SBR/Si composite.

For solid materials, there is an overall ^{1}H spin diffusion caused by the spatial transfer of the ^{1}H spin energy by flip-flop spin–spin transitions. Therefore, the observed T_1^H value from the benzene ring reflects not only the benzene ring molecular motion but also that of the other functional groups. The observed T_1^H rate ($1/T_1^H$) is equal to the intrinsic ^{1}H T_1^i rate and the ^{1}H spin diffusion rate, K_{SD} ($1/T_1^H = K_{SD} + 1/T_1^i$). In the SBR case, however, the observed T_1^H from the benzene ring differed from those obtained from the single and the double-bonded groups, especially at higher temperatures. This result indicates that the overall ^{1}H spin diffusion in SBR does not work efficiently, and we can employ the classical Bloembergen–Purcell–Pound theory[9] to analyze the observed T_1^H. Fast MAS also reduces the overall ^{1}H dipolar interaction (that is, ^{1}H spin diffusion) efficiently, so that the temperature dependence of the T_1^H curve in Figure 4 represents a liquid-like relaxation process that is governed by a pairwise ^{1}H dipolar interaction at higher temperatures.

T_1^H in the higher temperature region of Figure 4 is explained by a pairwise ^{1}H dipolar interaction with a distance of r (nm), as follows:[9,10]

$$\frac{1}{T_1^H} = f \cdot \frac{1.709\times10^5}{r^6\omega}\left(\frac{\tau\omega}{1+\tau^2\omega^2} + \frac{4\tau\omega}{1+4\tau^2\omega^2}\right) \tag{2}$$

where, τ is the correlation time of the molecular motion, ω is the Larmor frequency and f is a factor to fit the T_1^H minimum value observed. We assumed an isotropic high-frequency 180° flip motion for the benzene ring, which is combined with the overall main-chain rotational reorientation motion.[11] It is necessary to consider both the side-chain and main-chain motions for accurate estimation of the molecular motion. However, at higher temperatures, SBR performs like a liquid under higher frequency motion, so that we were not able to distinguish both motions from the temperature dependence of T_1^H alone. Figure 4 shows that the temperature dependence of T_1^H is apparently obeyed by a single isotropic correlation time at higher temperatures, although T_1^H can be rigorously explained by both motions. To determine the relationship between the apparent overall molecular motion and the pressure, we consider the apparent correlation time.

Figure 4 shows that the T_1^H minimum at 5.0 kHz MAS with the 3.2-mmϕ rotor is the smallest T_1^H of those obtained at any MAS rate. However, the T_1^H minimum at 2.13 kHz MAS with the 6.0-mmϕ rotor was the smallest. Its value was 0.61 s at $\sim$392 K. At such a high temperature, the ^{1}H spin diffusion effect in the SBR is negligibly small, even at slow MAS; consequently, the observed T_1^H minimum value can be calculated from Equation (2). The distance r is that of the ^{1}H pair, f = 1, and $\tau\omega$ = ca. 0.616. The molecular motion of the

SBR is also affected by the pressure, and it causes a change of the T_1^H minimum. Thus, the estimated r value is apparently the average values of the distances of all close ^{1}H pairs. We employed the value of 0.2 nm for the distance of the ^{1}H pair. This value is comparable to the averaged distance among the protons of the main chain in the SBR.

The T_1^H minimum at 4.26 kHz MAS with the 6.0-mmϕ rotor becomes larger than that obtained at 5 kHz MAS with the 3.2 mmϕ rotor. The ^{1}H–^{1}H dipolar interaction is usually reduced by increasing the MAS speed, so that the above result is contradictory for most polymers. If the ^{1}H spin diffusion is still active at temperatures >350 K, the T_1^H minimum at 5 kHz MAS should be larger than that at 4.26 kHz MAS. The pressure estimated from Equation (1) at 4.26 kHz MAS with the 6.0-mmϕ rotor is ca. 1.5 MPa. However, the pressure at 5 kHz MAS with the 3.2-mmϕ rotor is ca. 0.4 MPa, which is equal to the pressure at 2.13 kHz MAS with the 6.0-mmϕ rotor. The T_1^H minimum observed at 5 kHz MAS with the 3.2-mmϕ rotor is expected to be larger than that at 2.13 kHz MAS with a 6.0-mmϕ rotor because the influence of pressure on the molecular motion is the same, but the ^{1}H spin diffusion effect on T_1^H at 2.13 kHz MAS remains larger than that at 5 kHz MAS. However, because T_1^H at 4.26 kHz MAS with the 6.0-mmϕ rotor is also affected more by pressure than T_1^H at 5 kHz MAS with the 3.2-mmϕ rotor, the T_1^H minimum becomes larger than that at 5 kHz MAS with the 3.2-mmϕ rotor, although the MAS rate is slower. Furthermore, the T_1^H minimum gradually increases from a MAS rate of 5–20 kHz for the 3.2-mmϕ rotor. The increase of the MAS rate causes an increase of the inner pressure on the molecular motion of the SBR. The higher pressure causes stretching (rolling) of the SBR. Therefore, Figure 4 indicates that the increase of the T_1^H minimum is related to the degree of stretching (more precisely, it is related to the strain). These observations clearly suggest that the observed T_1^H, which is altered by molecular motion, is dominated by the centrifugal pressure.

The William–Landel–Ferry equation[12] for τ is employed to express the high-frequency molecular motion. The ^{1}H spin diffusion significantly affects the value of T_1^H at lower temperatures because of rigid molecular motion. Thus, we have only employed the William–Landel–Ferry equation to fit the value of T_1^H observed at higher temperatures. The William–Landel–Ferry equation is expressed with the correlation time τ_g at the glass-transition temperature T_g as follows:

$$\log\frac{\tau}{\tau_g} = \frac{-C_1\times(T-T_g)}{C_2+T-T_g} \qquad (3)$$

All temperature dependences of the T_1^H curves were fitted by the combination of Equations (2) and (3) for the higher temperature region. These fits are represented by the solid, dashed and two-dotted dashed lines in Figure 4. The T_g values of 250 K for both of the SBR/Si composites, obtained from differential scanning calorimetry measurements, were utilized. The parameters used are listed in Table 1 for 5–20 kHz MAS with the 3.2-mmϕ rotor. Figure 4 indicates that the observed T_1^H values in the temperature region >330 K are successfully explained by the combination of Equations (2) and (3).

Table 1 Parameters used for Equations (2) and (3) to fit the observed temperature dependence of T_1^H as shown in Figure 4[a]

MAS	C_1	C_2	τ_g[b]	f
5	3.47	270	2.58	0.979
10	3.47	270	2.58	0.907
15	3.47	270	2.58	0.875
20	3.47	270	2.58	0.830
25	4.32	180	9.92	0.852

Abbreviation: MAS, magic-angle spinning.
[a]Errors are within 5%.
[b]$\times 10^9$.

The T_1^H curves obtained under MAS rates of 5—20 kHz exhibit similar curvature. Thus, the parameters utilized are equivalent, except for the f value. This similarity indicates that the molecular motion related to T_1^H does not change significantly. In general, the T_1 minimum of the polymers (not only T_1^H) is not explained by the classical formula because the correlation time of the molecular motion is broadly distributed.[13,14] This distribution causes anisotropic motion so that the classical formula, which assumes isotropic motion, cannot adequately explain the T_1 minimum. In such a case, the temperature dependence curves of T_1 become significantly different from the simulated curve. However, Figure 4 shows that the observed T_1^H values at higher temperatures are in accordance with the simulated line. This result suggests that the molecular motion of the SBR can be assumed to be isotropic at higher temperatures. Therefore, the increase of the T_1^H minimum (the decrease of parameter f) indicates the effect of MAS. Specifically, it indicates the effect of the pressure on the molecular motion of the SBR. Furthermore, because the T_1^H curve does not change at each MAS rate, it is noted that the motional mode related to the T_1 relaxation process does not change significantly. This invariance is also suggested by the constancy of the parameters in Equation (3), which are listed in Table 1.

The temperature dependences of T_1^H observed at 4.26 and 8.51 kHz MAS, with the 6.0-mmϕ rotor also plotted in Figure 4. All of the T_1^H values measured at the MAS rates of 4.2, 6.4 and 8.5 kHz with the 6.0-mmϕ rotor and at 10 and 15 kHz with the 3.2-mmϕ rotor were observed to lie inside or along the dashed lines for both the *em*-SBR/Si and the *n*-SBR/Si composites. The difference between the observed T_1^H values was <50 ms. We refer to this area to as a moderate zone. The estimated pressures from Equation (1) using these MAS rates and rotors are between 1.5 and 6.1 MPa. Although the pressure at 8.5 kHz MAS with the 6.0-mmϕ rotor (6.1 MPa) is the same as that at 20 kHz with the 3.2-mmϕ rotor, the value of T_1^H observed at 8.5 kHz MAS with the 6.0-mmϕ rotor is smaller than that at 20 kHz with the 3.2-mmϕ rotor. This difference exists because the MAS speed of 8.5 kHz is not high enough to reduce the ^{1}H–^{1}H dipolar interaction, which is recoupled by the hindered molecular motion at a pressure of 6 MPa, even at higher temperatures. This observation also shows that moderate pressures of 1–6 MPa do not greatly influence the molecular motion related to T_1^H.

The T_1^H values observed at 25 kHz MAS exhibit different temperature dependence from those observed at 5–20 kHz MAS. The value of τ_g is estimated to be 9.92×10^{-9} s at 25 kHz MAS, whereas the value for 5–20 kHz MAS is 2.58×10^{-9} s. The correlation time at T_g becomes approximately four times longer than that at 5–20 kHz MAS. This result suggests that the molecular motion at 25 kHz MAS is strongly hindered and becomes slow. Furthermore, the temperature-dependent curves observed at 20 and 25 kHz MAS for the *em*-SBR/Si composite differed from those for the *n*-SBR/Si composite, while there was little difference between the end-chain-modified and -unmodified SBR at the other MAS rates.

To compare the difference in the temperature dependence of T_1^H between the *em*-SBR/Si and *n*-SBR/Si composites, we plotted the temperature-dependent curves of T_1^H for both composites at 20 and 25 kHz MAS in Figure 5. Both temperature dependences of T_1^H at 20 kHz MAS show a similar curve shape to those at 5–15 kHz MAS.

The parameters of the theoretical curves (gray colors) shown in Figure 5 are the same as those obtained for 5–15 kHz MAS, except for the *f* value. Interestingly, the temperature dependent $T_1{}^H$ curve for the *em*-SBR/Si composite is closer to the moderate zone than that obtained for the *n*-SBR/Si composite at both 20 and 25 kHz MAS. In addition, the τ_g value of the *em*-SBR/Si composite at 25 kHz MAS is 6.78×10^{-9} s. This value is less than that of *n*-SBR/Si composite (9.92×10^{-9} s). These results indicate that the hindrance induced by MAS on *em*-SBR is smaller than that induced on *n*-SBR in the SBR/Si composite, even under higher pressure conditions. This effect occurs because an interaction exists between the end-chain modifier and the silica filler. The phenomenon observed here resembles the depression of the storage and elastic moduli that is generally observed for normal rubbers containing fillers at higher strain, which is called the Payne effect.[15] Under fast MAS conditions, the bulk rubber in the sample rotor assumes a cylindrical shape. This transition means that the rubber is rolled by the pressure and incurs a large strain. The relationship between the storage modulus and strain for the *n*-SBR/Si composite shows a large Payne effect at strains >1%, compared with that for the *em*-SBR/Si composite (see graphical abstract). This difference suggests that the end-chain-modified SBR in the silica-filled composite does not yield to large strain amplitudes, whereas the unmodified SBR yields easily to high strains. Furthermore, the Payne effect appears discontinuously with the gradual increase of the strain. The storage modulus remains constant until 1% strain, but it decreases steeply as the strain increases past 1% (the critical strain amplitude). This phenomenon resembles the correlation time behavior observed at the fast MAS rate of 25 kHz, in which the correlation time becomes drastically slower from that at MAS rates <20 kHz. The steep change of the correlation time for molecular motion at 25 kHz MAS most likely reflects surpassing of the yield point of SBR/Si composites. Consequently, the temperature dependence of $T_1{}^H$ at higher MAS conditions gives information about the change of molecular motion that is observable at the macroscopic level. This relationship clearly suggests that the exertion of macroscopic pressure by MAS influences the microscopic molecular motion of rubbers, causing a change of $T_1{}^H$.

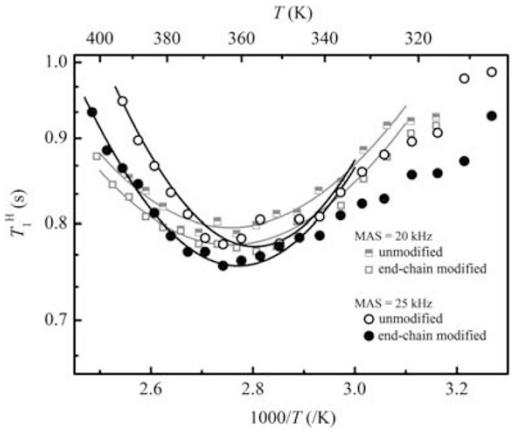

Figure 5 Comparison of the temperature dependence of $T_1{}^H$ between the end-chain-modified and the -normal (unmodified) SBR/Si composites at MAS rates of 20 and 25 kHz. The vertical axis is on a logarithmic scale.

Figure 4 shows the increment of $T_1{}^H$ depending on the MAS rate. The increment can be represented by the inverse of the factor *f*, 1/*f*. This value is related to the stretch ratio because higher MAS speeds cause greater centrifugal pressures, leading to rolled elongation. Therefore, the plot of the pressure as a function of 1/*f* should resemble the stress–strain relation. Figure 6 shows (a) the plot of the MAS pressure as a function of 1/*f* and (b) the stress–strain relation of the SBR/Si composites. Figure 6(a) clearly resembles (b), although the pressure is much smaller than stress. The elongation under fast MAS is different from the stress–strain process, but the rolling process by centrifugal pressure causes the SBR to deform against the stress applied. The molecular motion is affected similarly by a force during the MAS and stretching process. Therefore, we can conclude that $T_1{}^H$ under fast MAS is sensitive to changes of the molecular motion caused by stress.

CONCLUSIONS

We detected the increase in the FWHH of SBR at high temperatures and MAS speeds. The $T_1{}^H$ value increased with the MAS rate for

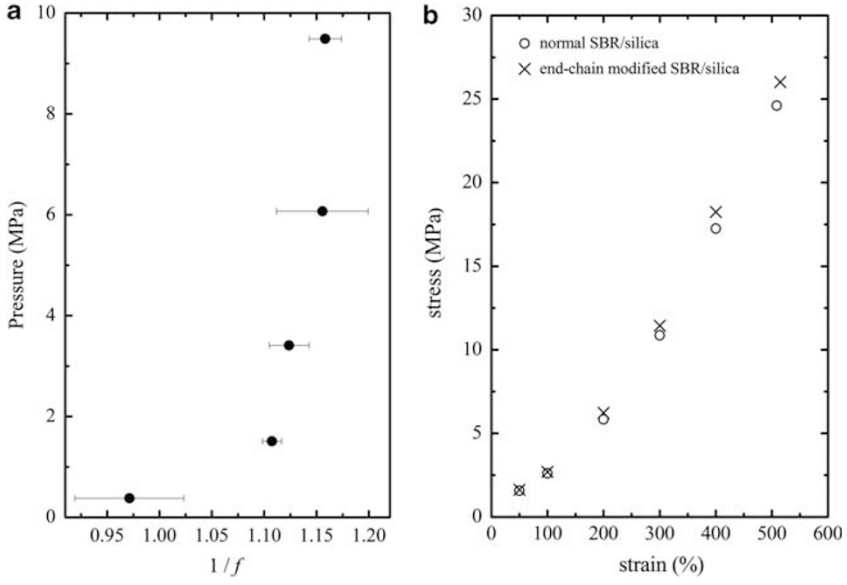

Figure 6 Comparison of (**a**) 1/*f* versus pressure and (**b**) the stress–strain curves of SBR/Si composites.

the SBR/Si composites. The plot of the inverse of f ($1/f$) versus the pressure estimated from the MAS speed exhibited a similar trend to that of the stress–strain curve. Furthermore, we observed that the temperature dependence of $T_1{}^{H}$ for the *em*-SBR/Si composite is different from that for the *n*-SBR/Si composite at higher MAS rates. This difference was attributed to the existence of an interaction between the silica filler and the SBR. We conclude that the value of $T_1{}^{H}$ under fast MAS is sensitive to physical and macroscopic properties. The value of $T_1{}^{H}$ is governed mainly by motion with the ^{1}H Larmor frequency; similarly, $T_1{}^{C}$ is related to the ^{13}C frequency, which is 1/4 of the ^{1}H frequency. In addition, the T_1 values in the rotating frame determine the frequency that mainly contributes to the physical deformation through relaxation experiments under MAS.

ACKNOWLEDGEMENTS

This work was completed with aid and cooperation from the Advanced Elastomer research group in the Society of Rubber Industry, Japan.

1 Kawamura, I., Kihara, N., Ohmine, M., Nishimura, K., Tuzi, S., Saito, H. Naito, A. Solid-state NMR studies of two backbone conformations at Tyr185 as a function of retinal configurations in the dark, light, and pressure adapted bacteriorhodopsins *J. Am. Chem. Soc.* **129,** 1016–1017 (2007).
2 Kawamura, I., Degawa, Y., Yamaguchi, S., Nishimura, K., Tuzi, S., Saito, H. Naito., A. Pressure-induced isomerization of retinal on bacteriorhodopsin as disclosed by fast magic angle spinning NMR. *Photochem. Photobio.* **83,** 346–350 (2007).
3 Van Geet, A. L. Calibration of methanol nuclear magnetic resonance thermometer at low temperature. *Anal. Chem.* **42,** 679–680 (1970).
4 Takahashi, T., Kawashima, H., Sugisawa, H. Baba, T. ^{207}Pb chemical shift thermometer at high temperature for magic angle spinning experiments. *Solid State Nuc. Magn. Reson.* **15,** 119–123 (1999).
5 Morikawa, A., Sone, T., Shibata, M. Tadaki, T. Modified solution SBR for the next generation. *Proceedings of IRC 2005*, 26-S1-I-01.
6 VanderHart, D. L., William, L. E. Garroway, A. N. Resolution in ^{13}C NMR of organic solids using high-power proton decoupling and magic-angle sample spinning. *J. Magn. Reson.* **44,** 361–401 (1981).
7 Rothwell, W. P. Waugh, J. S. Transverse relaxation of dipolar coupled spin systems under rf irradiation: Detecting motions in solids. *J. Chem. Phys.* **74,** 2721–2732 (1981).
8 Asano, A. Takegoshi, K. Free volume study of amorphous polymers detected by solid state ^{13}C NMR linewidth experiments. *J. Chem. Phys.* **115,** 8665–8669 (2001).
9 Bloembergen, N., Purcell, E. M. Pound, R. V. Relaxation effects in nuclear magnetic resonance absorption. *Phys. Rev.* **73,** 679–712 (1948).
10 McBrierty, V. J. Packer, K. J. *Nuclear Magnetic Resonance in Solid Polymers* (Cambridge Univ. Press, 1993) Chapters 2 and 3.
11 Schaefer, J., Sefcik, M. D., Stejskal, E. O., McKay, R. A., Dixon, W. T. Cais, R. E. Molecular motion in glassy polystyrenes. *Macromolecules* **17,** 1107–1118 (1984).
12 Williams, M. L., Landel, R. F. Ferry, J. D. The temperature dependence of relaxation mechanisms in amorphous polymers and other glass-forming liquids. *J. Am. Chem. Soc.* **77,** 3701–3707 (1955).
13 VanderHart, D. L. Garroway, A. N. ^{13}C NMR rotating frame relaxation in a solid with strongly coupled protons: Polyethylene. *J. Chem. Phys.* **71,** 2773–2787 (1979).
14 Lipari, G. Szabo, A. Model-free approach to the interpretation of nuclear magnetic resonance relaxation in macromolecules. 1. Theory and range of validity. *J. Am. Chem. Soc.* **104,** 4546–4559 (1982).
15 Payne, A. R. The dynamic properties of carbon black-loaded natural rubber vulcanizates. *J. Appl. Polym. Sci.* **6,** 57–63 (1962).